European Journal of Cell Biology 91 (2012) 800–808

Contents lists available at SciVerse ScienceDirect

European Journal of Cell Biology

journal homepage: www.elsevier.de/ejcb

A rod domain sequence in segment 1B triggers dimerisation of the two small *Branchiostoma* IF proteins B2 and A3

Anton Karabinos[a,*], Jürgen Schünemann[b], David A.D. Parry[c]

[a] SEMBID, s.r.o.-Research Center of Applied Biomedical Diagnostics, Hviezdoslavova 22, 08001 Prešov, Slovakia
[b] Max Planck Institute for Biophysical Chemistry, Department of Cellular Logistics, Am Fassberg 11, 37077 Goettingen, Germany
[c] Institute of Fundamental Sciences, Massey University, Palmerston North 4442, New Zealand

ARTICLE INFO

Article history:
Received 28 March 2012
Received in revised form 27 May 2012
Accepted 5 June 2012

Keywords:
Branchiostoma
Coiled coil
Heterodimer
Intermediate filament
Trigger motif

ABSTRACT

Previously, we cloned two *Branchiostoma* IF proteins A3 and B2 and demonstrated that both can form heteropolymeric IF based on a coiled coil dimer consisting of one B2 and one A3 polypeptide. In this study we continued in the characterisation of the B2/A3 heterodimer by searching for the sequences that play an important role in the triggering of the B2/A3 heterodimer. Using a series of deletion and chimeric B2, A3 and B1 constructs and the overlay assay as a tool, we were able to identify a part of the B2 sequence (segment 1A, linker L1 and the N-terminal part of segment 1B) which retains the ability of the full length protein B2 to specifically recognize A3 in blot overlays. Moreover, inspection of this A3-competent B2 fragment identified a short sequence in segment 1B which shares with the currently known trigger-like motif of cortexillin and other coiled coil proteins potential to form multiple inter-chain ionic interactions. Thus, a common and essential feature of trigger sequences with different primary structures found so far in IF and other coiled coil proteins seems to be their ability to form multiple inter-chain ionic interactions which brings the chains close to one another and allows coiled coil formation to propagate accordingly.

Introduction

There are about 70 different members of the IF family of proteins in man (Hesse et al., 2000, 2004) and, in vertebrates, these are subdivided into six types based on sequence similarities, gene structures, expression profiles and polymerisation properties (for reviews see Fuchs and Weber, 1994; Parry and Steinert, 1995; Herrmann et al., 2003, 2009). Keratins, which form epithelial filaments, are based on obligatory heteropolymeric double-stranded coiled coils and each molecule contains one type I and one type II chain. The type III chains include the four mesenchymally expressed proteins – desmin, vimentin, GFAP and peripherin – and these generally form homopolymeric IFs. The type IV classification includes the three neurofilament proteins and α-internexin, the type V group comprises the nuclear lamin proteins, and the two eye lens IF proteins – filensin and phakinin – represent the type VI chains. Orthologs of the vertebrate cytoplasmic type I to III IF proteins have also been found in early chordates (Karabinos et al., 1998, 2000; Luke and Holland, 1999; Wang et al., 2000, 2002).

The primary function of the cytoplasmic IF cytoskeleton seems to be resistance against mechanical stress, provided in large part in metazoan cells by the IF filamentous network. This view is supported by a variety of epidermal fragility syndromes induced by mutated human keratin genes (McLean and Lane, 1995), by knockout technology in mice (*i.e.* Hesse et al., 2000; Vijayaraj et al., 2009) as well as by reverse genetics in the nematode *C. elegans* (Karabinos et al., 2001b; Hapiak et al., 2003; Woo et al., 2004; Hüsken et al., 2008; Zhang et al., 2011).

Structurally, all IF proteins are similar. Each possesses a central rod domain characterized by α-helix-favouring heptad repeats. At its N- and C-terminal ends lie head and tail domains, respectively, that differ significantly in sequence both between chains and between chain types. The central rod domain is subdivided into segments 1A, 1B, 2A and 2B and these are connected to one another by the linkers L1, L12 and L2 respectively. However, the nuclear lamins and the cytoplasmic IFs from protostomia differ from the cytoplasmic IFs of vertebrates, cephalochordates and urochordates as each contains a longer rod domain due to the insertion of an additional 42 residues (six heptads) in segment 1B. In addition, the nuclear lamins have a unique tail containing an Ig-like segment, a nuclear localisation signal and, in most cases, a CaaX box (Erber et al., 1999). It seems reasonable to assume that lamins represent an ancestor sequence of cytoplasmic IFs (Fuchs and Weber, 1994; Parry and Steinert, 1995; Erber et al., 1998; Herrmann et al., 2003).

The structure of the rod domain in IF molecules enables them to assemble both *in vitro* and *in vivo* into one of four closely related 10 nm-like filaments (Fuchs and Weber, 1994; Parry and Steinert, 1995; Herrmann et al., 2003, 2009). Formation of the

* Corresponding author. Tel.: +421 905 402 683.
E-mail address: sembid.pp@gmail.com (A. Karabinos).

0171-9335/$ – see front matter © 2012 Elsevier GmbH. All rights reserved.
http://dx.doi.org/10.1016/j.ejcb.2012.06.001

double-stranded coiled coil is driven by internalisation of the apolar residues in positions *a* and *d* of the heptad repeats. The last ten years has revealed significant progress in the elucidation of the atomic structure of the vimentin coiled coil (Strelkov et al., 2002; Meier et al., 2009; Nicolet et al., 2010). However, the elementary question, regarding the trigger mechanism through which coiled coil propagation is initiated in the IF coiled coil remains an open one. In order to provide insight into this process Wu et al. (2000) searched for trigger motifs within keratin K5/K14. These authors prepared a series of point substitutions in both chains and tested their ability to form filaments both *in vitro* and *in vivo*. In addition, they tested the stability of particular dimers and tetramers using a urea disassembly assay. This resulted in the identification of two trigger-like motifs. The first was located on the largely conserved C-terminal end of 2B and this was thought likely to be a common feature in all IF chains. The second motif identified in this study was located in the C-terminal half of coil 1, specifically between residues 79 and 91 of segment 1B. Interestingly, no trigger-like motif was found in segment 1A (Wu et al., 2000).

Previously, we cloned and characterized 13 cytoplasmic IFs from cephalochordate *Branchiostoma.* Five proteins were identified as bona fide keratins. This assignment was confirmed by the obligatory heteropolymeric filament formation of the recombinant proteins. Any stoichiometric mixture of type I (k1, Y1, E1) and type II (D1, E2) proteins provided IF. In addition, two of the *Branchiostoma* type I keratins formed chimeric IF when mixed with human type II keratin 8 (Karabinos et al., 2000). Three keratins (k1, Y1, D1) and protein X1 are the only IF proteins expressed in the gastrula. The number of lancelet IF proteins increases at the neurula and early larval stages to 7 and 11 respectively, and in the adult 13 different proteins have been found. The keratins are the major IF proteins in the *Branchiostoma* nerve cord. Proteins X1, C1 and C2 possess some keratin-like characters and were shown to be integrated into the epidermal and neuronal keratin meshwork (Karabinos et al., 2001a). Finally, the last currently known *Branchiostoma* IF proteins A1, A2, A3, B1 and B2 formed a separated A/B branch in the evolutionary trees and were proposed to be lancelet-specific (Karabinos et al., 2002). The B1 protein is expressed in mesodermally derived muscle tails and in coelomic epithelia, and is also able to form homopolymeric IF *in vitro*. In contrast, its closest relative B2 is co-expressed with the three homologous proteins A1-A3 in the intestinal epithelia. It can form heteropolymeric IF with A3 essential in the formation of filaments, based on a coiled coil dimer consisting of one B2 and one A3 polypeptide. Interestingly, both IF proteins A3 and B2, which have been previously cloned from the *Branchiostoma floridae*, essentially lack a tail domain and are designated therefore as "small" (Karabinos et al., 2002).

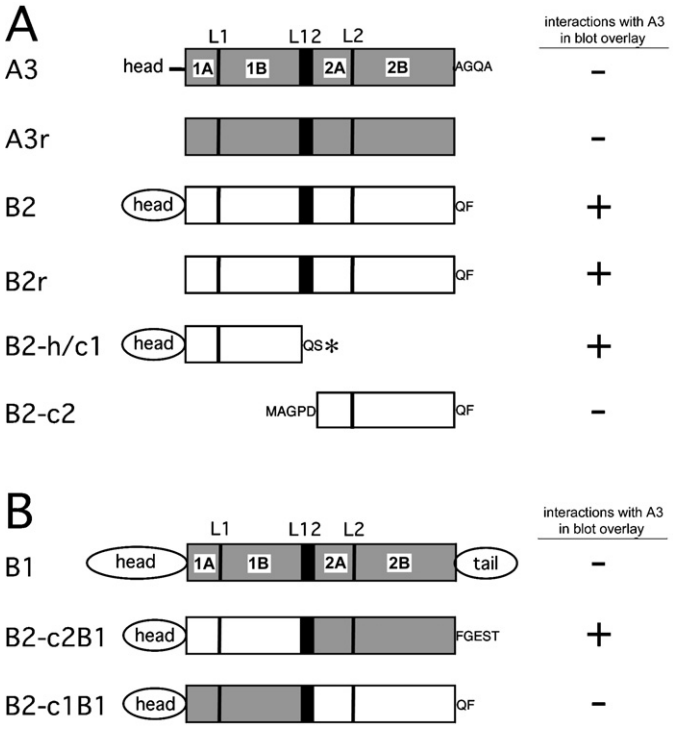

Fig. 1. Schematic representation of the *Branchiostoma* proteins A3, B2, B1 and the corresponding deletion and chimeric mutants used in this study. The structural organisation of an IF protein consists of a head, a rod and a tail domain, as indicated. The helical rod covers segments 1A, 1B, 2A and 2B which are connected by linkers L1, L12 and L2. The plus (+) and minus (−) characters on the right summarize the ability of the corresponding biotin-labelled proteins and mutants to interact with the protein A3 in blot overlays. (A) The fragments A3r and B2r represent the rod domains of the corresponding A3 and B2 proteins. The B2-h/c1 and B2-c2 fragments are deletion mutants of B2 that lack the entire coil 2 and coil 1 segment, respectively. Note the four (AGQA) and two (QF) residue long tail in the full-length A3 and B2 proteins, respectively (Karabinos et al., 2002). The fragment B2-c2 starts with the five residues "MAGPD" which are derived from the linker L12. The asterisk on the B2-h/c1 deletion mutant represents an 24 extra residues (described in Fig. 5A) derived from the expression vector pET. (B) In the chimeric B2-c1B1 and B2-c2B1 mutants the B2 coil 1 and coil 2 segment, respectively, are replaced by the corresponding part of the protein B1. The B2-c2B1 chimeric mutant ends with the four residues FGES derived from the B1 tail and the threonine that is attached to the sequence due to a cloning strategy.

In this study we continued in the characterisation of the B2/A3 heterodimer by searching for the sequences that are responsible for early and highly specific B2/A3 interactions *in vitro*. Such sequences would be expected to play an essential role in the triggering of the B2/A3 heterodimer. Using a series of deletion and chimeric B2, A3 and B1 constructs and the overlay assay as a tool, we were able to identify a part of the B2 sequence (segment 1A, linker L1 and the N-terminal part of segment 1B) which retains the ability of the full length protein B2 to specifically recognize A3 in blot overlays. Moreover, inspection of the A3-competent B2 fragment identified a putative trigger-like sequence in segment 1B that closely resembles the currently defined trigger-motif of cortexillin I and other coiled coil proteins.

Results

Preparation of recombinant proteins and protein mutants

B2 and A3 form a double-stranded coiled coil dimer containing one B2 and one A3 chain. The B2/A3 heterodimerisation represents the first step in the assembly process of these proteins that subsequently ends in the formation of long 10 nm thick IFs *in vitro* (Karabinos et al., 2002). The early and highly specific B2/A3 interactions are best documented in the blot overlay assay (Karabinos et al., 2002). In order to find segments and/or motifs that are responsible for early and highly specific B2/A3-interactions we prepared, expressed and purified a series of deletion and chimeric mutants of B2 and A3 proteins (see Fig. 1). In addition, the full-length protein B1 was expressed and included in this study as a control. The first two deletion mutants B2r and A3r represent the rod domains of the corresponding proteins. The B2-h/c1 deletion mutant contains only the whole head, the coil 1 rod segment and the first two QS residues of linker L12 (Fig. 1A). Moreover, this fragment is terminated by an additional 24 residues derived from the expression vector (depicted by the asterisk in Fig. 1A; see also Fig. 5A). The B2 deletion mutant B2-c2 contains the entire coil 2 segment flanked N-terminally by the linker L12 residues AGPD and C-terminally by the two residue long tail (Fig. 1A). The B2 chimeric mutant B2-c2B1 contains the entire linker L12 but with the coil 2 rod segment replaced by the corresponding B1 sequence terminated by the five residues

Table 1
Physical parameters of *Branchiostoma* proteins and fragments used in this study.

Protein or protein fragment	Number of amino acid residues	Molecular weight[a]	Isoelectric point (p*I*)[a]
A3	335	37,407	5.55
A3r	309	34,584	5.15
B2	350	39,609	4.77
B2r	307	35,074	4.62
B2-h/c1	206	23,277	5.24
B2-h/c1-p1	123	13,982	5.16
B2-h/c1-p2	82	9226	5.37
B2-h/c1-p3	15	1561	12.20
B2-c2	154	17,513	4.89
B2-c1B1	348	39,883	4.82
B2-c2B1	357	40,871	4.63
B1	464	51,299	5.05

[a] The values were calculated using the GCG software package program PEPTIDESORT.

FGEST in the B1 tail (Fig. 1B). In the second B2 chimeric mutant B2-c1B1, the entire coil 1 rod segment, together with the six head SGEKRE and the three linker L12 QSQ residues, is replaced by the corresponding B1 sequences (Fig. 1B). The proteins and mutants were recombinantly expressed and purified to homogeneity by ion exchange chromatography in a urea solution (see 'Methods' section). Some physical parameters of the described proteins and mutants are provided in Table 1.

B2 coil 1 rod segment specifically binds A3 in blot overlay

Recombinant proteins and mutants, described above, were biotin-labelled and their binding activities were analysed in the blot overlay assay (see summary in Fig. 1). As documented in Fig. 2, the biotin-labelled A3-rod fragment A3r specifically decorated B2, B2r and B2-h/c1 on the membrane thereby indicating that the head domains of both A3 and B2 proteins are not necessary for these interactions. Interestingly, no interactions between the A3r probe and the B2-c2 mutant, which represent the coil 2 rod segment of protein B2, were seen. Similar results were obtained in the reciprocal experiments using the biotin-labelled B2r, B2-h/c1 and B2-c2 fragments as probes. While the former two specifically bind A3 and A3r proteins in the blot overlay, no interactions were seen for the biotinylated B2-c2 probe (Fig. 2). Thus, the coil 1 domain seems to be the only part of the protein B2 that is necessary for early and specific interactions with protein A3 in blot overlays.

In order to confirm different A3-binding competence for the B2 coil 1 and coil 2 segments, as described above, their activities were analysed again in blot overlays using the two chimeric mutants B2-c1B1 and B2-c2B1. In these chimeras both the B2 coil 1 and B2 coil 2 segments, respectively, were put within the context of the full length IF molecule. This domain swap kept the heptad repeat containing helices undisrupted and gives them better conditions for optimal folding (see for example Chou et al., 1992). The B2-c1B1 biotin-labelled probe, in which the coil 1 segment was replaced by the corresponding B1 region, recognizes only B1 of 10 different *Branchiostoma* IFs fixed on the membrane (Fig. 3). This chimeric mutant resembles interaction properties of the biotin-labelled homopolymeric protein B1 used in the same assay as the control (Fig. 3). This is true also for the B2-c2B1 chimeric mutant, consisting of the B2 head and coil 1 domains combined with the B1 coil 2 that, however, also decorated the protein A3 (Fig. 3). The B2-c2B1 protein behaves in this assay like the true chimera retaining the A3-binding competence of B2 and simultaneously exhibiting the B1 interactions of the protein B1 (Fig. 3).

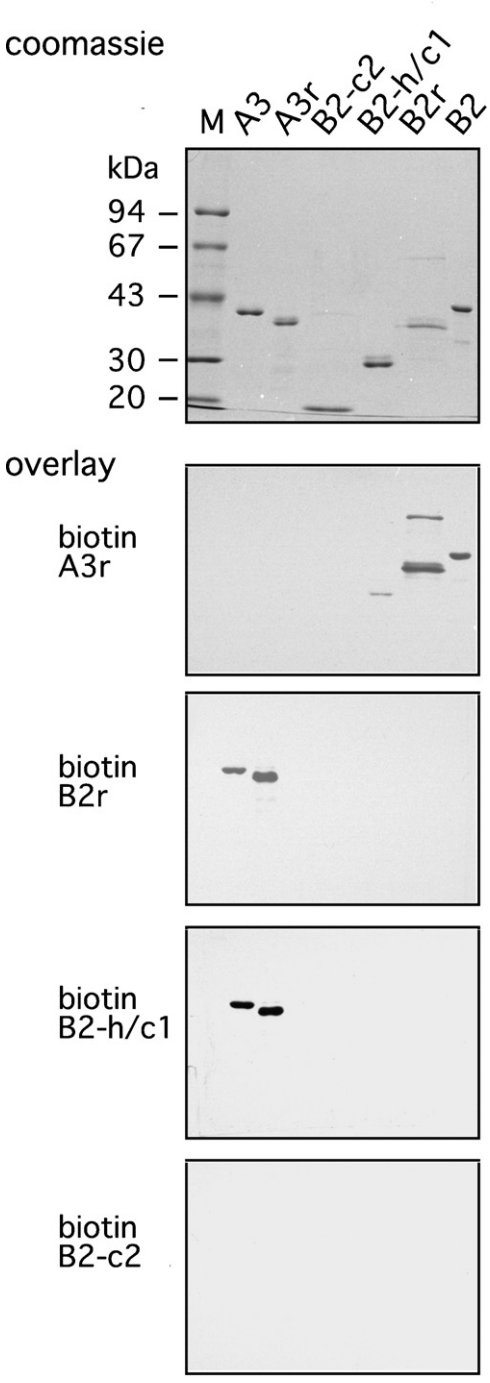

Fig. 2. Blot overlay assays of the biotin-labelled A3r, B2r, B2-h/c1 and B2-c2 deletion mutants. Approximately equal amounts of purified recombinant *Branchiostoma* proteins A3 and B2 as well as the four deletion mutants A3r, B2-c2, B2-h/c1 and B2r were separated by SDS PAGE and either stained with Coomassie brilliant blue (the upper panel) or transferred to nitrocellulose membranes for overlay experiments. The lower panels show the results of the overlays using biotin-labelled protein probes, as indicated on the left. Note the specific interactions of the A3r probe with B2, B2r and B2-h/c1 while no interactions were observed with the B2-c2, A3 and A3r polypeptides that are fixed on the membrane. There is also a strong decoration of both A3 and A3r recombinant proteins by the biotin-labelled B2r and B2-h/c1 probes in contrast to the B2-c2 probe that failed to show any binding on the membrane. Marker proteins (M) and an approximate molecular mass standard in kDa are shown on the left of the upper panel.

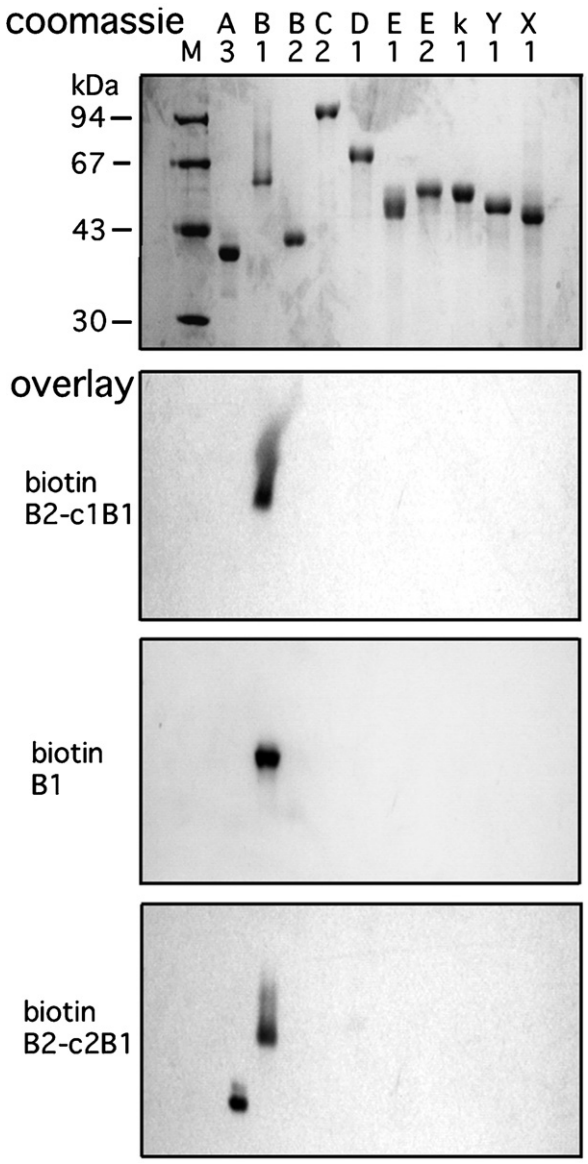

Fig. 3. The blot overlay search for interactions of the biotin-labelled B2-c2B1 and B2-c1B1 chimeric mutants as well as the protein B1 with ten blotted immobilized *Branchiostoma* IF proteins. Equal amounts of the ten *Branchiostoma* purified recombinant proteins A3, B1, B2, C2, D1, E1, E2, k1, Y1 and X1 (indicated at the top of the upper panel) were separated by SDS-PAGE and either stained with Coomassie brilliant blue (upper panel) or transferred on to nitrocellulose membranes for overlay assays. The lower panels show results of the corresponding blot overlay experiments using the biotin-labelled B2-c1B1, B1 or B2-c2B1 probe as marked on the left. Note the exclusive decoration of the protein B1 by the biotinylated B2-c1B1 and B1 probes in contrast to the biotin-labelled B2-c2B1 that, in addition, decorates the protein A3. Marker proteins (M) and an approximate molecular mass standard in kDa are shown on the left of the upper panel.

Thus, the coil 1 segment of the B2-c2B1 chimera is responsible for the A3-specific interactions in blot overlays in contrast to the coil 2 domain of the B2-c1B1 chimera that does not reveal any binding activities.

Interaction incompetent B2-c2 fragment reveals usual circular dichroism spectra

In order to directly exclude possibilities that the incompetence of the B2-c2 fragment to bind A3, documented above, is not due to a wrong protein folding, the B2-c2 polypeptide was investigated by circular dichroism (CD) spectroscopy. As shown in Fig. 4A this

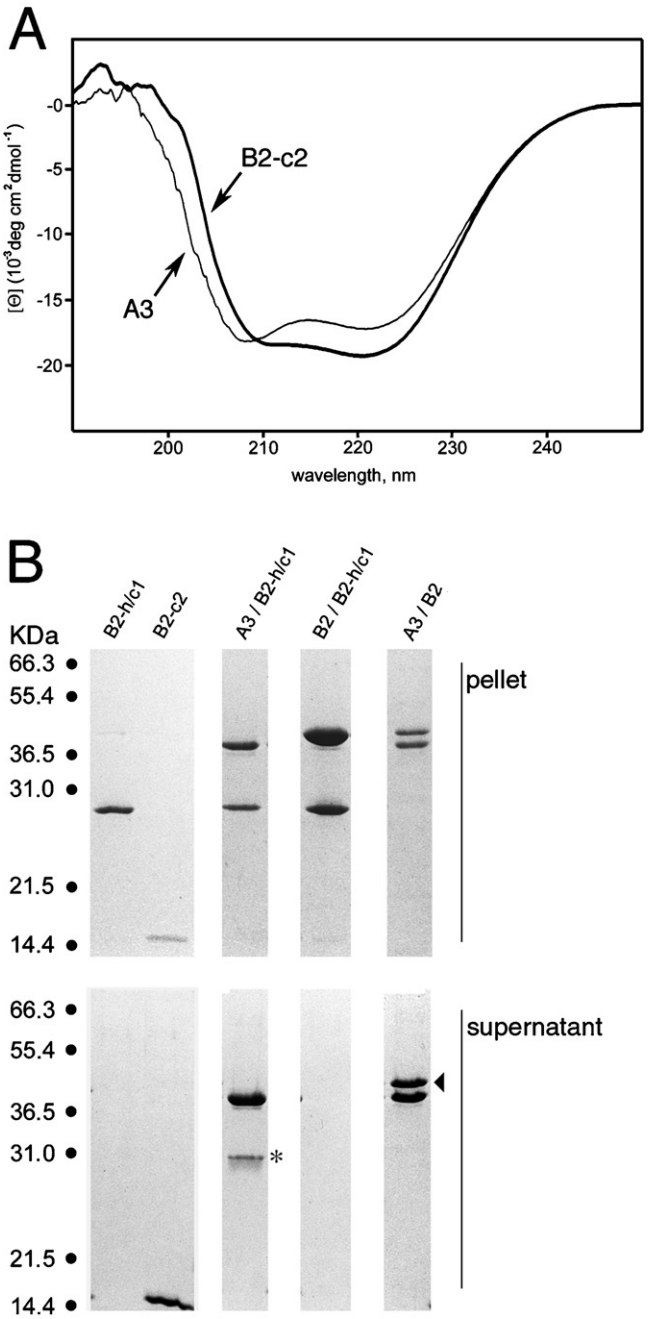

Fig. 4. (A) Circular dichroism spectroscopy (CD) of the B2 deletion mutant B2-c2 and the full-length recombinant protein A3. These analyses revealed typical α-helical absorption spectra for both proteins. The calculated α-helical contents of A3 and B2-c2 proteins were approximately 35%. (B) Interactions between the B2-h/c1 and A3 polypeptides are also detected in the urea-free buffer. The recombinant proteins B2, A3 and the B2 deletion mutants B2-h/c1 and B2-c2 were dialysed, either alone or in mixtures, from the urea-containing into the urea-free buffer, centrifuged and aliquots of the pelleted and the supernatant fractions were analysed by SDS-PAGE for appearance of the corresponding protein bands (see 'Methods' section for details). The recombinant proteins B2 and B2-h/c1, either alone or in mixture, highly aggregate in the urea-free buffer as documented by the appearance of corresponding bands exclusively in pellets (upper panel). The solubility of both B2 polypeptides in the urea-free buffer increased dramatically upon mixing with the partner protein A3, as documented by the appearance of the corresponding protein bands in the supernatants of the A3/B2-h/c1 and A3/B2 mixtures (lower panel). Since the second B2 deletion mutant B2-c2 was highly soluble in the urea-free buffer its analysis in a similar way to that described for the fragment B2-h/c1 was not possible. The approximate molecular mass standard in kDa are given on the left of both panels.

analysis revealed typical α-helical absorption spectra for the B2-c2 fragment and an α-helical content of about 35%. This was highly similar to the CD characteristics of the full-length protein A3, measured under similar experimental conditions (Fig. 4A). Thus, the normal looking α-helical absorption spectra of the B2-c2 fragment argues against the possibility that incorrect folding of the B2-c2 fragment was responsible for the A3-interaction incompetence in the blot overlay experiments, described above (Figs. 2 and 3).

B2 coil 1 rod segment specifically binds A3 also in urea free buffer

In order to independently verify behaviour of the B2-h/c1 fragment we tested its ability to bind A3 in the urea-free buffer. This assay was based on our observations that the recombinant protein B2 alone forms only non-specific aggregates in such buffers. However, in a mixture with A3 its solubility dramatically increased, probably as the result of the formation of specific B2/A3 complexes (our unpublished results and Fig. 4B).

Thus, the B2-h/c1 and B2-c2 fragments were first dialysed, either alone or in mixtures, from the urea-containing buffer into the 10 mM Tris, pH 9, buffer containing 200 mM NaCl and 1 mM 2-mercaptoethanol. The insoluble material was centrifuged and the aliquots of resulting pellets and supernatants were analysed by SDS-PAGE for appearance of the corresponding protein bands. As shown in Fig. 4B the B2-h/c1 fragment alone or in the mixture with B2 (used as a negative control) was completely insoluble, as revealed by the appearance of the corresponding protein bands exclusively in pellets. In contrast, the solubility of B2-h/c1 dramatically increased in mixture with the protein A3, as revealed by the appearance of the B2-h/c1 protein band in the corresponding supernatant (Fig. 4B). Unfortunately, a similar investigation on the B2-c2 fragment was not possible because this fragment was highly soluble in the urea-free buffer (Fig. 4B).

Thus, the presence of A3, but not B2, prevents aggregation of the B2-h/c1 fragment in the urea-free buffer which indicates the ability of the B2 coil 1 rod segment to interact specifically with A3 under different experimental conditions. This provides independent support for the results of the blot overlay experiments, described above.

Sub-segment of the B2 coil 1 specifically binds A3 in blot overlay

In order to check which parts of the B2 coil 1 interact with the protein A3, we chemically cleaved the A3-binding competent and biotin-labelled B2-h/c1 fragment at the two internal cysteines (marked by "X" in Fig. 5A) using the 2-nitro-5-cyanobenzoic acid (see 'Methods' section for details). The three resulting peptides B2-h/c1-p1, B2-h/c1-p2 and B2-h/c1-p3 are presented in Fig. 5A. The former two peptides were purified to homogeneity by ion-exchange chromatography and the relative rate of biotinylation was checked in a western blot using the streptavidin-peroxidase assay. The smallest peptide B2-h/c1-p3 contains only 15 residues derived from the expression plasmid (Fig. 5A).

As shown in Fig. 5B the largest peptide B2-h/c1-p1, that contains the head, segment 1A, linker L1 and forty residues from segment 1B (Fig. 5A), was strongly biotinylated in contrast to the labelling of B2-h/c1-p2 which was not sufficient for use as a probe in blot overlays (Fig. 5B). The blot overlay experiment using the B2-h/c1-p1 biotinylated peptide as a probe clearly demonstrated the ability of this fragment to interact specifically with the protein A3 immobilized on the membrane (Fig. 5C). Thus, the latter experiment as well as all of the other experiments described above collectively mapped the segment 1A, linker L1 and the forty residue long piece of segment 1B as the minimal B2 sequence required for highly specific interactions to occur with protein A3 *in vitro*.

Segment 1B of proteins B2 and A3 contains a putative trigger-like motif

A trigger motif has been identified in the heptad-containing rod domain in several coiled coil proteins. The currently defined motif of the actin-bundling protein cortexillin I and some other coiled coil proteins is the 13-residue sequence "xxLExchxcxccx" in which "x", "c" and "h" refer to a variable, a charged and a hydrophobic residue, respectively (Kammerer et al., 1998). Inspection of the A3-binding competent coil 1 segment of B2 and the corresponding part of A3 proteins has failed to find such an element in these sequences (Fig. 5A). It is known, however, that charged residues often occupy positions *a* and *d* of the heptads in trigger sequences, and that these are involved in both intra-and inter-helical salt-bridges (Burkhard et al., 2000). We found one region with this characteristic in segment 1B for both B2 and A3 chains (marked by horizontal lines in Fig. 5A). In these heptads no less than 5 and 4 a positions as well as 3 and 1 *d* positions of the B2 and A3 sequences, respectively, are occupied by charged (K,R,E) or non-hydrophobic (T,S,C,N,Q) residues. In addition, two other neighbouring *d* positions contain the bulky residue tryptophan (marked by "W" in Fig. 5A). Interestingly, both tryptophans are also found in the *Branchiostoma* A1 and A2 proteins in contrast to all other currently known *Branchiostoma* IF (see Karabinos et al., 2000, 2002 and in Fig. 6A). A detailed inspection of the mentioned heptads in the B2 and A3 segment 1B sequences mapped six charged residues in positions *g* and *a* (marked with arrows in Fig. 5A) and these have potential for multiple inter-helical salt bridges of the *g-aĭ* and *a-gĭ* type (indicated with double arrows in Fig. 5A). The first of these is the A3Lys85 which could interact with glutamic acids at positions 101 and 108 in the B2 sequence. Two other charged residues B2Arg109 and A3Arg92 lie in positions *a* and exhibit the potential to form salt bridges with the A3Glu91 and B2Glu108, respectively, both occupying a *g* position. The latter residue B2Glu108 could simultaneously interact with A3Lys85, as mentioned above (Fig. 5A). In addition, four other potential salt bridges of the classical *g-eĭ* and *e-gĭ* type were identified in both coil 1 sequences (depicted in Fig. 5A).

Thus, we have identified here a potential binding competent sequence (*i.e.* a trigger-like motif) in segment 1B for both B2 and A3 chains. This motif is of the form "−+xxxxx−+" ("−", "+" and "x" refer to negatively charged, positively charged and variable residue, respectively). This resembles the currently defined trigger-motif of cortexillin I and other coiled coil proteins in that it has the potential to form multiple salt bridges (Kammerer et al., 1998; Burkhard et al., 2000). It is reasonable to speculate, that this trigger-like motif could, at least in part, be responsible for the initiation/triggering of the specific B2/A3 interactions, demonstrated in our *in vitro* experiments (Figs. 1–5).

Discussion

Intermediate filaments belong to a large group of proteins that are characterised by a common heptad-containing rod domain but with head and tail domains that are chemically and structurally diverse. The heptad substructure provides a means by which oligomerisation may occur and, in the case of the IF proteins, the formation of double-stranded coiled coils. However, this process is initiated in many coiled coil structures by an autonomous 13-residue long trigger motif (Kammerer et al., 1998; Burkhard et al., 2000). In order to identify such motif(s) in the IF sequences Wu et al. (2000) made a series of point substitutions within the keratins K5/K14. They then mixed various combinations of the wild-type and mutant chains *in vitro* to examine the stability of the reconstituted dimers and/or tetramers in the urea disassembly assay. Using this approach Wu et al. found two motifs that were essential for the

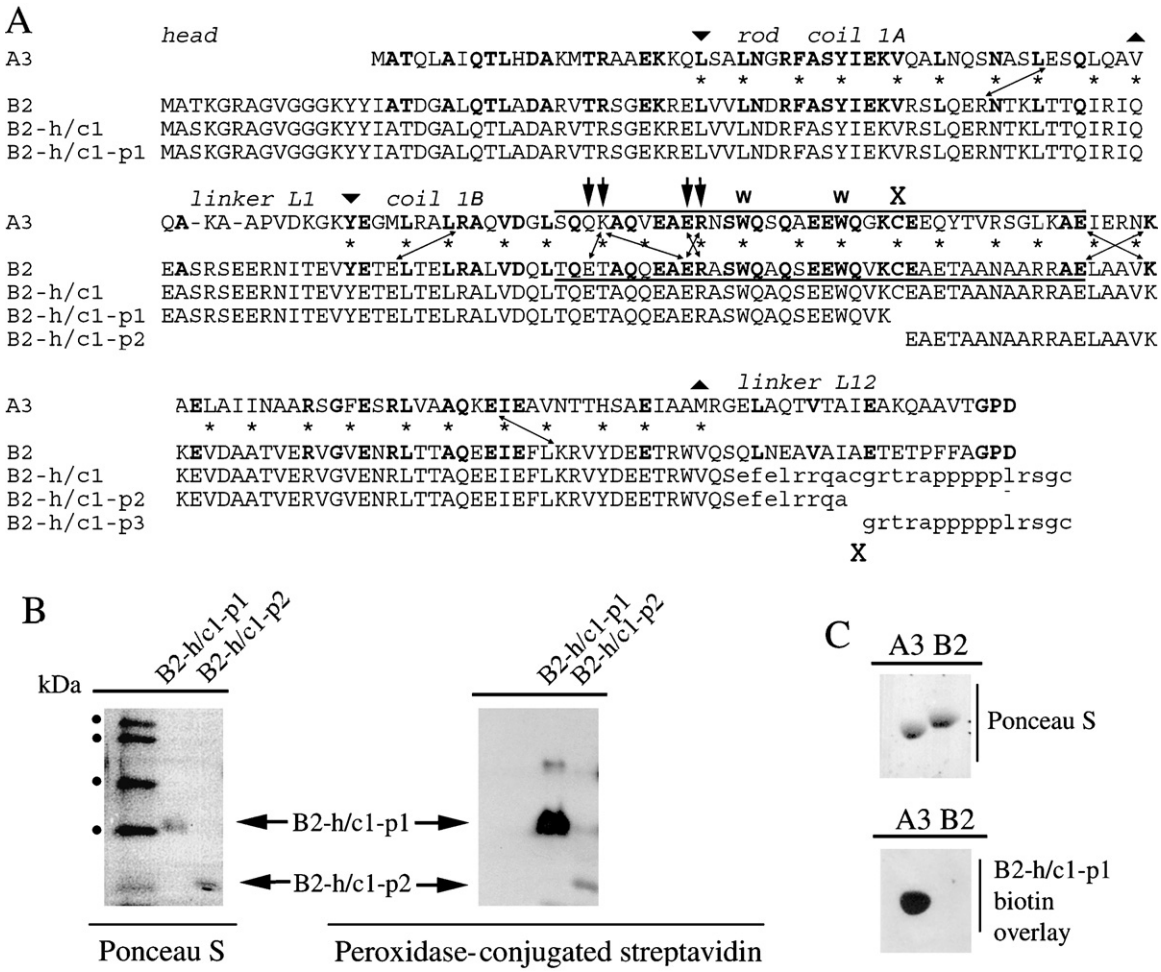

Fig. 5. (A) Alignment of the head and coil 1 amino acid sequences of the *Branchiostoma* proteins A3 and B2 and the four B2 fragments B2-h/c1, B2-h/c1-p1, B2-h/c1-p2 and B2-h/c1-p3. The head, coil 1 and the linker L12 are indicated. Arrows pointing downwards and upwards mark the beginning and the end of the rod segments 1A and 1B. Asterisks between the rod segments of A3 and B2 proteins mark the *a* and *d* positions of the heptad repeat pattern. Dashes are used to optimize the sequence alignment. Bold letters indicate identical residues in the A3 and B2 sequences. The region of heptad repeats lacking the usual numbers of apolar residues in the *a* and *d* positions in segment 1B in the A3 and B2 chains are marked by two horizontal lines. The four arrows mark the positions of the six charged residues in segment 1B which are involved in potential *g-aï* and *a-gï* salt bridges, indicated by double arrows (see text for details). The two capital letters "W" and one "X" shown above the sequences indicate positions of the two tryptophan and one cysteine residue, respectively. The cysteine residue was used for chemical cleavage of the B2-h/c1 fragment resulting in three peptides B2-h/c1-p1, B2-h/c1-p2 and B2-h/c1-p3. The latter is only 15 residues long, and is derived from the expression plasmid due to a cloning strategy. (B) The relative level of biotin-labelling of the purified B2-h/c1-p1 and B2-h/c1-p2 peptides determined by western blotting. Equal amounts of the purified and biotin-labelled peptides were separated by SDS-PAGE and stained with Ponceau S (left panel) or transferred to the nitrocellulose membrane for peroxidase-conjugated streptavidin staining (right panel) as indicated. The B2-h/c1-p1 peptide was strongly labelled in this peroxidase-conjugated streptavidin assay in contrast to a weak staining of the peptide B2-h/c1-p2. Approximate molecular mass standard in kDa is given at the left of the left panel. (C) The biotin-labelled B2-h/c1-p1 peptide strongly stains A3 in the blot overlay (lower panel). The upper panel shows the control nitrocellulose membrane with both transferred A3 and B2 proteins, stained with Ponceau S as indicated.

stability of the coiled coil molecules. The first motif was found in the conserved helix termination motif in segment 2B and it was suggested that it might function in a similar manner in all IF chains. The second potential trigger motif was identified in the C-terminal part of segment 1B. However, the authors did not find any trigger activity in segment 1A or in any other parts of the rod (Wu et al., 2000).

We searched here for trigger-like motifs in the two small *Branchiostoma* IF proteins B2 and A3. Both proteins are co-expressed in the intestinal epithelium and some other tissues of the developing and adult *Branchiostoma*. Together, they form a regular, double-stranded B2/A3 coiled coil *in vitro* (Karabinos et al., 2002). First, we prepared five deletion and two chimeric mutants for B2 and A3 proteins (Figs. 1 and 5A) and tested the ability of individual mutants to specifically recognize recombinant proteins in blot overlays. Using this very powerful approach to demonstrate early and specific heterotypic interactions between B2 and A3 proteins (Karabinos et al., 2002) we identified segment 1A, linker L1 and the first forty residues in segment 1B as the minimal B2 sequence required for specific interactions with A3 *in vitro* (Figs. 2, 3, 4B and 5C). Thus, the heads and the coil 2 segments do not seem to be involved in the early and specific interactions between the B2 and A3 proteins *in vitro*.

The inability of the B2 coil 2 segment to interact with A3 in blot overlays (Figs. 2 and 3) was somewhat surprising. The coil 2 rod segment represents the longest coiled coil region in IF proteins (Fuchs and Weber, 1994; Parry and Steinert, 1995; Nicolet et al., 2010) and the B2-c2 fragment, used as a probe in the blot overlays, seemed to be correctly folded as indicated by CD spectroscopy (Fig. 4A). There are several possible explanations for this finding. Firstly, the absence of the trigger-like activity in the coil 2 segment might be specific to B2 and A3 proteins which might contain trigger-like sequences only in their coil 1 segment. Such an interpretation would indicate important differences between the latter two proteins and the homologous homopolymeric protein B1 (Karabinos et al., 1998) since in this latter case the protein B1

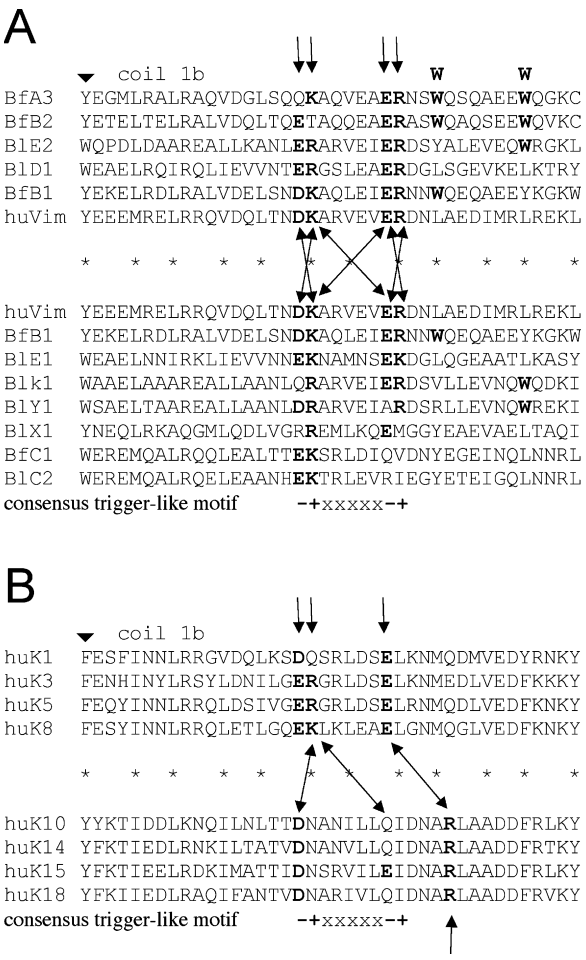

Fig. 6. (A) Sequence alignment of the first forty residues in segment 1B of the *Branchiostoma* A3 and B2 proteins together with the corresponding parts of other *B. floridae* (Bf)/*B. lanceolatum* (Bl) IF proteins as well as human vimentin. Arrows pointing down mark the start of segment 1B and asterisks mark the *a* and *d* positions of the heptad repeat pattern. The four arrows above the sequences mark the putative trigger-like motif "−+xxxxx−+" of the B2 and A3 proteins, that is called and serves as a "consensus trigger-like motif" for the all aligned sequences. Residues of the aligned sequences that fit the charged positions of the "consensus trigger-like motif" are indicated in bold. Note the presence of the "consensus trigger-like motif" in the homopolymeric *Branchiostoma* protein B1 and human vimentin that has the potential to form six *g-aĭ* and *a-gĭ* type salt bridges; indicated by double arrows. This is in contrast to the four such bridges that could be formed by the "consensus trigger-like motif" between the B2 and A3 sequences (see Fig. 5A and text for details). The "consensus trigger-like motif" also has the potential to form six *g-aĭ* and *a-gĭ* type salt bridges in the *Branchiostoma* keratin heterodimers E1/E2 and E1/D1 while only four and three such connections could potentially be formed in the keratin heterodimers containing k1 and Y1 proteins, respectively. Note that there is also much less conservation of the consensus-type motif in the *Branchiostoma* proteins X1, C1 and C2 that are considered to be lancelet-specific/keratin associated IFs with a currently unknown mode of assembly (Karabinos et al., 2000, 2002). The capital letters "W" above the aligned sequences mark the two neighbouring tryptophan residues in positions *a* which are conserved within the *Branchiostoma* proteins A1, A2 (Karabinos et al., 2002), A3 and B2 and are indicated in bold. (B) Sequences of the four selected human type I and type II keratins aligned as described in the panel A. The three arrows above the sequences mark the first three positions of the charged residues of the "consensus trigger-like motif" "−+xxxxx−+", as described in panel A. All residues in keratins that fit the "consensus trigger-like motif" are indicated in bold. Notice there are only two to three charged residues fitting the "consensus trigger-like motif" in the type II keratins K1, K3, K5 and K8 while only one to two such residues are conserved in type I keratins K15 and K10, K14, K18. There is also the possibility of an additional salt bridge (marked with the double arrow) of the *g-eĭ* type that involves the glutamic acid of the type II keratins and the conserved arginine of the type I keratins, marked with an arrow below the sequences.

in blot overlays is able to self-interact with both the coil 1 segment of the chimeric protein B2-c1B1 as well as the coil 2 segment of the B2-c2B1 chimera (Fig. 3). Moreover, human keratins K5/K14 exhibit some trigger-like and/or stabilisation-properties in the coil 2 segment (Wu et al., 2000). A second possible interpretation of the binding incompetence of the B2 coil 2 could be that it was not observable using the particular experimental approach used here. This might be because a) a putative trigger-like sequence in coil 2 was blocked due to biotinylation of lysines and/or because b) partial SDS-denaturation of the proteins fixed on overlay membranes compromised interactions of the B2-c2 fragment in the blot overlay experiments (Figs. 2 and 3). Thus, additional experiments and a different approach will be needed to answer the question of whether the formation of the B2/A3 coiled coil dimer is triggered by the coil 1 segment alone, as indicated in this study, or whether it is also mediated by other sequence-motifs, not identified in the present study.

The currently defined trigger motif characterised in several coiled coil proteins has the signature "xxLExchxcxccx" in which "x", "h" and "c" refers for a variable, an hydrophobic and a charged residue, respectively (Kammerer et al., 1998; Burkhard et al., 2000). Inspection of the interaction-competent B2 and A3 coil 1 fragments failed to identify this motif. Nonetheless, contiguous heptads were found in the segment 1B sequences of B2 and A3 proteins (Fig. 5A) in which the six residues – A3Lys85, A3Glu91, A3Arg92, B2Glu101, B2Glu108 and B2Arg109 – lie in either *g* or *a* positions and could form multiple salt bridges (indicated by double arrows in Fig. 5A) resembling those of the currently defined trigger-motif (Kammerer et al., 1998; Burkhard et al., 2000). We defined this sequence element with the signature "−+xxxxx−+" ("−", "+" and "x" refer to negatively charged, positively charged and variable residue, respectively) as a putative trigger-like motif that could, at least in part, be responsible for the initiation of the B2/A3 interactions and the triggering of the coiled coil structure. Interestingly, this motif reveals some conservation in diverse IF proteins including the *Branchiostoma* keratins and protein B1 as well as the human homopolymeric protein vimentin (Fig. 6A). It is, nonetheless, much less conserved in human keratins in which only one *a-gĭ* and one *g-aĭ* salt bridge would be expected between the corresponding type I and type II sequences as well as one classical *g-eĭ* salt bridge (Fig. 6B). In general, however, we think that there need not be a trigger sequence motif common to all IF. Rather, it might be strongly advantageous if different chain combinations have different trigger sequences, thereby helping to ensure that inappropriate sequences did not heterodimerise. A trigger sequence should, perhaps, be best thought of as having the potential to form multiple inter- and intra-chain ionic interactions, thereby bringing the chains close to one another and allowing coiled coil formation to propagate accordingly.

Human vimentin, unlike other IF proteins, has been extensively studied crystallographically and a near complete crystal structure has been determined for its rod domain. However, while the structures of segment 1A and the coil 2 structures of vimentin are known (Strelkov et al., 2002; Meier et al., 2009; Nicolet et al., 2010) details of the structure of segment 1B have yet to be reported. These data, as well as crystallization experiments involving other IF proteins, are expected to bring new insight into the role of a putative trigger-like motif, defined in this study, in segment 1B of the IF coiled coil structure in Branchiostoma B2/A3.

Methods

Nucleic acid techniques

Deletion mutants A3r, B2r, B2-h/c1 and B2-c2 of the proteins A3 and B2 were prepared by cloning of the corresponding PCR

fragments amplified from the *B. floridae* A3 and B2 cDNAs (Karabinos et al., 2000) into the pET23a expression vector. For the preparation of the chimeric construct B2-c1B1 the *Age*I restriction site was initially introduced into the B2 cDNA/pET23a cloning vector using the QuiaChange mutagenesis kit (Stratagene). Next the entire coil 1 segment was removed from the B2 cDNA/pET23a vector using the *Bst*EII/*Age*I restriction enzymes and replaced by the corresponding coil 1 PCR fragment amplified from the *B. floridae* B1 cDNA (Karabinos et al., 1998). The chimeric fragment B2-c2B1 was prepared by digestion of the *Age*I-site-containing B2 cDNA/pET23a (described above) using the restriction enzymes *Age*I/*Bsu*36I. This was followed by PCR amplification and *Age*I/*Bsu*36I digestion of the corresponding coil 2 segment of B1 cDNA and cloning into the B2 cDNA/pET23a. The primers used for preparation of the deletion and chimeric mutants, described above, are available upon request. All DNA constructs were sequenced to ensure that the correct deletion or chimeric proteins were generated.

Protein techniques

Expressions, purifications and *in vitro* assembly assays of the recombinant full length, deletion and chimeric mutant proteins were as described (Karabinos et al., 1998, 2000, 2002).

Biotinylation of recombinant proteins and overlay assays were essentially as described (Karabinos et al., 2002). Briefly, the blot overlay assays were performed in 20 mM Tris, pH 7.5 buffer containing 4 M urea and 1 mM 2-mercaptoethanol. After incubation with a biotin-labelled probe and the subsequent wash the nitrocellulose membranes were treated with horse-radish peroxidase-conjugated streptavidin (Pierce, Rockford, IL, USA) and developed using the ECL chemiluminescence kit (Thermo Fisher Scientific Inc., Waltham, MA, USA).

Binding properties of the B2-h/c1 fragment in the urea-free buffer were analysed as follows. Recombinant proteins A3, B2, B2-h/c1 and B2-c2 at a concentration of 0.8 mg/ml in urea buffer were dialysed either alone or in mixtures for 20 h at room temperature against 10 mM Tris, pH 9, buffer containing 200 mM NaCl and 1 mM 2-mercaptoethanol. This was followed by centrifugation at 18,000 × *g* for 10 min. The pelleted protein aggregates were stored at −20 °C while the soluble supernatant fractions were precipitated with chloroform/methanol (1:4, v/v). Aliquots of the pelleted and precipitated supernatant protein fractions were separated on 12% SDS-PAGE and visualized by Coomassie staining.

Circular dichroism measurements were performed on a Jasco J 720 spectropolarimeter (Japan Spectroscopic Co., Ltd., Tokyo, Japan) using the cuvette with path length of 0.2 cm. The 10 mM Tris, pH 9 buffer containing 250 mM NaCl and 0.2 mM 2-mercaptoethanol was used. The circular dichroism was expressed as the molar ellipticity, calculated using the protein concentration, determined by a Bradford assay. The relative α-content was calculated using the molar ellipticity at 208 nm (Greenfield and Fasman, 1969) using the k2d software for protein secondary structure prediction (Andrade et al., 1993).

Cleavage of the biotinylated B2-h/c1 protein fragment was achieved by a chemical method using the 2-nitro-5-thiocyanobenzoic acid (NCTB; Jacobson et al., 1973), briefly as follows. The recombinant biotinylated protein B2-h/c1 was dissolved in 8 M urea, 10 mM Tris buffer, pH 8. Approximately five-fold molar excess of NCTB (Sigma; N-7009) over total thiol groups was added. After 3 h at 37 °C, the mixture was subjected to ion exchange chromatography on Mono S and Mono Q as described (Karabinos et al., 2000). The obtained peptide fractions were either precipitated with acetone and assayed on SDS-PAGE using a tricine running system or used as probes in blot overlay assays. Direct automated Edman degradation of the isolated B2-h/c1-p2 peptide was not possible due to the blocking of the N-terminus by an iminothiazolidinyl residue (Jacobson et al., 1973).

Acknowledgements

This work was performed in part at the Max Planck Institute for Biophysical Chemistry in Göttingen. We thank Klaus Weber for discussions.

Appendix A. Supplementary data

Supplementary data associated with this article can be found, in the online version, at http://dx.doi.org/10.1016/j.ejcb.2012.06.001.

References

Andrade, M.A., Chacon, P., Merelo, J.J., Moran, F., 1993. Evaluation of secondary structure of proteins from UV circular dichroism spectra using an unsupervised learning neural network. Protein Eng. 6, 383–390.
Burkhard, P., Kammerer, R.A., Steinmetz, M.O., Bourenkov, G.P., Aebi, U., 2000. The coiled-coil trigger site of the rod domain of cortexillin I unveils a distinct network of interhelical and intrahelical salt bridges. Structure 8, 223–230.
Chou, K.-C., Maggiora, G.M., Scheraga, H.A., 1992. Role of loop helix interactions in stabilising four helix bundle proteins. Proc. Natl. Acad. Sci. U.S.A. 89, 7315–7319.
Erber, A., Riemer, D., Bovenschulte, M., Weber, K., 1998. Molecular phylogeny of metazoan intermediate filament proteins. J. Mol. Evol. 47, 751–762.
Erber, A., Riemer, D., Hofemeister, H., Bovenschulte, M., Stick, R., Panopoulou, G., Lehrach, H., Weber, K., 1999. Characterisation of the Hydra lamin and its gene; a molecular phylogeny of metazoan lamins. J. Mol. Evol. 49, 260–271.
Fuchs, E., Weber, K., 1994. Intermediate filaments: structure, dynamics, function and disease. Annu. Rev. Biochem. 63, 345–382.
Greenfield, N., Fasman, G.D., 1969. Computed circular dichroism spectra for the evaluation of protein conformation. Biochemistry 8, 4108–4116.
Hapiak, V., Hresko, M.C., Schriefer, L.A., Saiyasisongkhram, K., Bercher, M., Plenefisch, J.D., 2003. mua6, a gene required for tissue integrity in *Caenorhabditis elegans*, encodes a cytoplasmic intermediate filament. Dev. Biol. 263, 330–342.
Herrmann, H., Hesse, M., Reichenzeller, M., Aebi, U., Magin, T.M., 2003. Functional complexity of intermediate filament cytoskeletons: from structure to assembly to gene ablation. Int. Rev. Cytol. 223, 83–175.
Herrmann, H., Strelkov, S.V., Burkhard, P., Aebi, U., 2009. Intermediate filament: primary determinants of cell architecture and plasticity. J. Clin. Invest. 119, 1772–1783.
Hesse, M., Franz, T., Tamai, Y., Taketo, M.M., Magin, T.M., 2000. Targeted deletion of keratin 18 and 19 leads to trophoblast fragility and early embryonic lethality. EMBO J. 19, 5060–5070.
Hesse, M., Zimek, A., Weber, K., Magin, T.M., 2004. Comprehensive analysis of keratin gene clusters in humans and rodents. Eur. J. Cell Biol. 83, 19–26.
Hüsken, K., Wiesenfahrt, T., Abraham, Ch., Windoffer, R., Bossinger, O., Leube, R.E., 2008. Maintenance of the intestinal tube in *Caenorhabditis elegans*: the role of the intermediate filament protein IFC-2. Differentiation 76, 881–896.
Jacobson, G.R., Schaffer, M.H., Stark, G.R., Vanaman, T.C., 1973. Specific chemical cleavage in high yield at the amino peptide bonds of cysteine and cystine residues. J. Biol. Chem. 248, 6583–6591.
Kammerer, R.A., Schulthess, T., Landwehr, R., Lustig, A., Engel, J., Aebi, U., Steinmetz, M.O., 1998. An autonomous folding unit mediates the assembly of two-stranded coiled coils. Proc. Natl. Acad. Sci. USA 95, 13419–13424.
Karabinos, A., Riemer, D., Erber, A., Weber, K., 1998. Homologues of vertebrate type I, II and III intermediate filament (IF) proteins in an invertebrate; the IF multigene family of the cephalochordate *Branchiostoma*. FEBS Lett. 437, 15–18.
Karabinos, A., Riemer, D., Panopoulou, G., Lehrach, H., Weber, K., 2000. Characterisation and tissue-specific expression of the two keratin subfamilies of intermediate filament proteins in the cephalochordate *Branchiostoma*. Eur. J. Cell Biol. 79, 1–10.
Karabinos, A., Wang, J., Wenzel, D., Panopoulou, G., Lehrach, H., Weber, K., 2001a. Developmentally controlled expression pattern of intermediate filament proteins in the cephalochordate *Branchiostoma*. Mech. Dev. 101, 283–288.
Karabinos, A., Schmidt, H., Harborth, J., Schnabel, R., Weber, K., 2001b. An essential role for four intermediate filament proteins in *Caenorhabditis elegans* development. Proc. Natl. Acad. Sci. U.S.A. 98, 7863–7868.
Karabinos, A., Schunemann, J., Parry, D.A.D., Weber, K., 2002. Tissue-specific co-expression and in vitro heteropolymer formation of the two small *Branchiostoma* intermediate filament proteins A3 and B2. J. Mol. Biol. 316, 127–137.
Luke, G.N., Holland, P.W., 1999. Amphioxus type I keratin cDNA and the evolution of intermediate filament genes. J. Exp. Zool. 285, 50–56.
McLean, W.H., Lane, E.B., 1995. Intermediate filaments in disease. Curr. Opin. Cell Biol. 7, 118–125.
Meier, M., Padilla, G.P., Herrmann, H., Wedig, T., Hergt, M., Patel, T.R., Stetefeld, J., Aebi, U., Burkhard, P., 2009. Vimentin coil 1A – a molecular switch involved in the initiation of filament elongation. J. Mol. Biol. 390, 245–261.
Nicolet, S., Herrmann, H., Aebi, U., Strelkov, S.V., 2010. Atomic structure of vimentin coil 2. J. Struct. Biol. 170, 369–376.

Parry, D.A.D., Steinert, P.M., 1995. Intermediate Filament Structure. Springer, New York.

Strelkov, S.V., Herrmann, H., Geisler, N., Wedig, T., Zimbelmann, R., Aebi, U., Burkhard, P., 2002. Conserved segments 1A and 2B of the intermediate filament dimer: atomic structures and role in filament assembly. EMBO J. 21, 1266.

Vijayaraj, P., Kröger, K., Reuter, U., Windoffer, R., Leube, R.E., Magin, T.M., 2009. Keratins regulate protein biosynthesis through localization of GLUT1 and -3 upstream of AMP kinase and Raptor. J. Cell Biol. 187, 175–184.

Wang, J., Karabinos, A., Schünemann, J., Riemer, D., Weber, K., 2000. The epidermal intermediate filament proteins of tunicates are distant keratins; a polymerisation-competent hetero coiled coil of the *Styela* D protein and Xenopus keratin 8. Eur. J. Cell Biol. 79, 478–487.

Wang, J., Karabinos, A., Zimek, A., Meyer, M., Riemer, D.S., Hudson, C., Lemaire, P., Weber, K., 2002. Cytoplasmic intermediate filament protein expression in tunicate development; a specific marker for the test cells. Eur. J. Cell Biol. 81, 302–311.

Woo, W.-M., Goncharov, A., Jin, Y., Chisholm, A.D., 2004. Intermediate filaments are required for *C. elegans* epidermal elongation. Dev. Biol. 267, 216–229.

Wu, K.C., Bryan, J.T., Morasso, M.I., Jang, S.I., Lee, J.H., Yang, J.M., Marekov, L.N., Parry, D.A.D., Steinert, P.M., 2000. Coiled coil trigger motifs in the 1B and 2B rod domain segments are required for the stability of keratin intermediate filaments. Mol. Biol. Cell 11, 3539–3558.

Zhang, H., Landmann, F., Zahreddine, H., Rodriguez, D., Koch, M., Labouesse, M., 2011. A tension-induced mechanotransduction pathway promotes epithelial morphogenesis. Nature 471, 99–103.